

Constrained H-Phe-Phe-NH₂ Analogues with High Affinity to the Substance P 1–7 Binding Site and with Improved Metabolic Stability and Cell Permeability

Rebecca Fransson,[†] Christian Sköld,[†] Jadel M. Kratz,^{‡,||} Richard Svensson,^{‡,⊥} Per Artursson,^{‡,⊥,#} Fred Nyberg,[§] Mathias Hallberg,[§] and Anja Sandström^{*,†}

[†]Department of Medicinal Chemistry, Uppsala University, Box 574, SE-751 23 Uppsala, Sweden

[‡]Department of Pharmacy, Uppsala University, Box 580, SE-751 23 Uppsala, Sweden

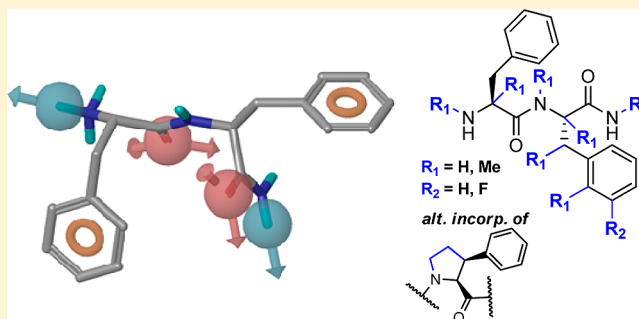
[§]Department of Pharmaceutical Biosciences, Uppsala University, Box 591, SE-751 24 Uppsala, Sweden

^{||}Programa de Pós-Graduação em Farmácia, Centro de Ciências da Saúde, Departamento de Ciências Farmacêuticas, Universidade Federal de Santa Catarina, 88.040-900, Florianópolis, SC, Brazil

[⊥]The Uppsala University Drug Optimization and Pharmaceutical Profiling Platform (UDOPP), Chemical Biology Consortium Sweden (CBCS), Uppsala University, Box 580, SE-751 23 Uppsala, Sweden

[#]Science for Life Laboratory, Uppsala University, SE-751 23 Uppsala, Sweden

ABSTRACT: We recently reported the discovery of H-Phe-Phe-NH₂ as a small and high affinity ligand for the substance P 1–7 (SP_{1–7}, H-Arg-Pro-Lys-Pro-Gln-Gln-Phe-OH) specific binding site and its intriguing ability to reduce neuropathic pain. With the overall aim to develop stable and orally bioavailable SP_{1–7} mimetics, the dipeptide was chosen as a lead compound. Herein the structure–activity relationship (SAR) of a set of modified H-Phe-Phe-NH₂ analogues is presented together with their potential active uptake by PEPT1 transporter, intestinal permeability, and metabolic stability. Local constraints via peptide backbone methylation or preparation of cyclized analogues based on pyrrolidine were evaluated and were shown to significantly improve the *in vitro* pharmacokinetic properties. The SAR was rationalized by deriving a plausible binding pose for the high affinity ligands. Rigidification using a 3-phenylpyrrolidine moiety in the C-terminal of H-Phe-Phe-NH₂ resulted in high affinity and improved intrinsic clearance and intestinal epithelial permeability.



INTRODUCTION

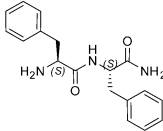
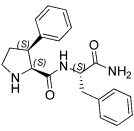
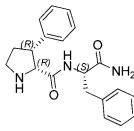
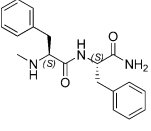
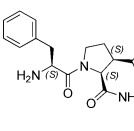
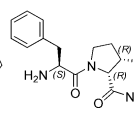
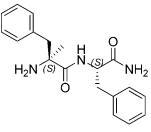
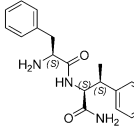
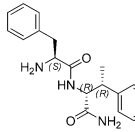
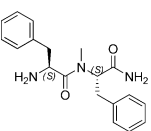
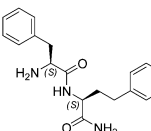
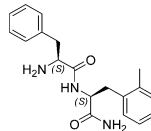
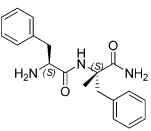
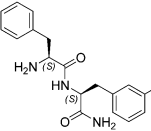
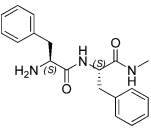
The undecapeptide substance P (SP, H-Arg-Pro-Lys-Pro-Gln-Gln-Phe-Phe-Gly-Leu-Met-NH₂)¹ is a neurotransmitter and neuromodulator in the central and peripheral nervous system and is most well-known for its involvement in pain. It belongs to the tachykinin family and constitutes the endogenous ligand for the neurokinin-1 (NK-1) receptor.^{2,3} SP is degraded into several bioactive fragments of which the N-terminal metabolite SP 1–7 (SP_{1–7}, H-Arg-Pro-Lys-Pro-Gln-Gln-Phe-OH) is the most abundant.^{4–6}

SP_{1–7} has been shown to reverse naloxone provoked opioid tolerance and withdrawal, in contrast to SP and its C-terminal fragments that amplify these effects.^{7–9} It has also been demonstrated that SP_{1–7} attenuates the inflammatory¹⁰ and the nociceptive¹¹ effects exerted by SP. Moreover, it was recently observed that SP_{1–7} induces antihyperalgesia in diabetic mice, suggesting a possible influence on neuropathic pain.¹² We find this observation particularly interesting, since no satisfactory treatment of neuropathic pain is available today.¹³ The effects of SP_{1–7} are suggested to be mediated through an indirect

activation of the naloxone-sensitive sigma receptor (σ_1) system.¹² SP_{1–7} itself is, however, not an active ligand for the σ_1 receptor nor do the biological effects observed for SP_{1–7} appear to be mediated through any of the known tachykinin or opioid receptors.¹² Even though the inhibitory effect of SP_{1–7} on SP induced behavior can be reversed by the nonselective opioid ligand naloxone, specific antagonists for the opioid receptors (μ , δ , and κ) do not inhibit this effect.^{14,15} More likely, the effects of SP_{1–7} are generated via an as yet undefined macromolecular target at specific binding sites identified for this heptapeptide in rat and mouse spinal cord and brain.^{16–18} Although most studies on SP_{1–7} have been done in rodents, its relevance in humans is suggested from the presence of SP and SP degrading enzymes in human and the presence of this heptapeptide fragment in human cerebrospinal fluid (CSF).^{19,20}

Received: February 8, 2013

Table 1. Binding Affinity of H-Phe-Phe-NH₂ Analogues to the SP₁₋₇ Binding Site

Compound	$K_i \pm \text{S.E.M}$ (nM)	Compound	$K_i \pm \text{S.E.M}$ (nM)
	8.4 ± 0.4^a		33.9 ± 2.5^c
1			50.5 ± 1.5^c
	189 ± 3		$2.2^{c, d}$
2			93.1 ± 0.2^c
	70.4 ± 3.0		17.5 ± 0.8^c
3			68.0 ± 1.2^c
	9.4 ± 0.1^b		6.2 ± 0.2
4			11.5 ± 0.1
	26.0 ± 1.2		3.3 ± 0.2
5		12	
	136 ± 2		
6			

^a K_i value determined at the same occasion as for 2–12. A K_i value of 1.5 nM was achieved in a previous run using other batches of membrane and labeled ligand, as reported previously.²³ ^bSubmitted sample contained compound 4 along with the ring closed form (i.e., the diketopiperazine) in a 92:8 relationship. ^cCorrespondence to each diastereomers undetermined. ^d8a (2:1 ratio of 8a and 8b), evaluated in triplicate at six concentrations in each run.

We previously reported a structure–activity relationship (SAR) study of the heptapeptide toward the specific binding site that revealed that the first four N-terminal amino acids in SP₁₋₇ are not essential for binding, since each could be substituted with an alanine or removed without significantly affecting the affinity.²¹ Interestingly, amidation of the C-terminal of SP₁₋₇ resulted in a peptide with greater binding affinity toward the SP₁₋₇ binding site compared to the native heptapeptide ($K_i = 0.3$ nM and $K_i = 1.6$ nM, respectively). In analogy with the binding studies it was found that the amidated analogue of SP₁₋₇ was more potent than SP₁₋₇ in reducing abstinence symptoms in morphine dependent rats and in inducing antihyperalgesia in diabetic mice.^{8,22}

In parallel with the SAR investigation of SP₁₋₇, similar studies were performed on the endogenous μ -receptor agonist endomorphin-2 (EM-2, H-Tyr-Pro-Phe-Phe-NH₂).²³ The interest in this tetrapeptide originates from the observations by Botros et al.¹⁷ that endomorphin-1 (EM-1, H-Tyr-Pro-Trp-Phe-NH₂) and EM-2 interact with the SP₁₋₇ binding site. However, a significant difference in binding affinity between the two tetrapeptides was observed. EM-1 and EM-2 displayed a 1000-fold and a 10-fold lower affinity, respectively, compared to the endogenous ligand SP₁₋₇. From an alanine scan and truncation study of EM-2 the same SAR as for SP₁₋₇ was observed. The C-terminal was shown to be crucial for binding affinity to the SP₁₋₇ binding site, and substitution of either of

the two amino acids in the N-terminal with alanine resulted in only small differences in affinity. Truncation of EM-2 resulted in identification of the dipeptide H-Phe-Phe-NH₂ (**1**) possessing a K_i of 1.5 nM.²³ Notably, **1** was recently shown to attenuate the signs of hyperalgesia, allodynia, and nociception in diabetic mice after intrathecal administration, in a similar manner compared to peptide SP₁₋₇ and its amidated analogue.²⁴ Dipeptide (**1**) is therefore clearly a very promising starting point for the development of future agents for the treatment of neuropathic pain.

Given the interesting results obtained from **1**, we felt prompted to further optimize this lead compound into stable and orally bioavailable SP₁₋₇ mimetics. Herein we report the synthesis and SAR of a set of constrained H-Phe-Phe-NH₂ analogues evaluated in a binding assay displacing [³H]SP₁₋₇. In addition a plausible binding conformation of the high affinity ligands was generated and the potential active uptake by the PEPT1 transporter, intestinal permeability, and metabolic stability of the dipeptide analogues were investigated.

RESULTS

Biological Evaluation. The dipeptides **1–12** in Table 1 were prepared using solid-phase peptide synthesis. The compounds were evaluated in a binding assay using spinal cord membrane from Sprague–Dawley rats and radioactive [³H]SP₁₋₇ as tracer.¹⁷ The binding affinities of compounds **1–12** for the SP₁₋₇ binding site are summarized in Table 1.

Methylation of the peptide backbone giving analogues **2**, **3**, **5**, and **6** resulted in lower affinity in general (K_i = 26–189 nM) except for compound **4**, which maintained similar affinity as **1** (K_i of 9.4 and 8.4 nM, respectively). Rigidification of the N-terminal phenylalanine using a pyrrolidine analogue resulted in reduced binding affinities (**7a** and **7b**, K_i = 33.9–50.5 nM). However, corresponding rigidification of the C-terminal phenylalanine gave **8a** and **8b**, of which one diastereomer showed improved binding affinity (K_i = 2.2 nM) and one diastereomer lower binding affinity (K_i = 93 nM). Because of a difficult separation, the diastereomer **8a** could not be completely isolated from diastereomer **8b**, which hence was evaluated in a 2:1 ratio of **8a** and **8b**. However, from the binding affinity difference one can still conclude that diastereomer **8a** has a significantly better binding affinity compared to **8b**. A methyl group on the β -carbon in the C-terminal side chain as in compounds **9a** and **9b** reduced the binding affinity 2–8 times. Elongation of the side chain with one carbon gave compound **10**, which showed similar affinity to compound **1**. Furthermore, small modifications on the aromatic part of the C-terminal phenylalanine were well tolerated (cf. **1** with **11** and **12**).

In Vitro Metabolic Stability. The metabolic stability was determined by incubating the compounds with pooled human liver microsomes (HLM). In vitro half-life ($t_{1/2}$) and in vitro intrinsic clearance (Cl_{int}) were calculated using previously published models, and the results are presented in Table 2.^{25,26} The Cl_{int} is used to rank compounds with regard to metabolic stability. It can give a good indication of the in vivo hepatic clearance when the overall clearance mechanism is metabolic and when oxidative metabolism dominates (i.e., $Cl_{metabolic} \gg Cl_{renal} + Cl_{biliary} + Cl_{other}$). The following cutoff values were used to classify the compounds with regard to metabolic stability: $Cl_{int} < 47 \mu L \min^{-1} mg^{-1}$ indicates a low risk for high first pass metabolism in vivo, $47 < Cl_{int} < 92$ a moderate risk, and $Cl_{int} > 92$ a high risk.²⁷

Table 2. Metabolic Stability Data of Compounds **1–12**^a

compd	Cl_{int}^b ($\mu L \min^{-1} mg^{-1}$)	$t_{1/2}^c$ (min)
1	121 \pm 39	12 \pm 4
2	2.7 \pm 1.5	597 \pm 40
3	64 \pm 11	22 \pm 4
4	92 \pm 0	15 \pm 1
5	38 \pm 15	40 \pm 16
6	175 \pm 5	7.9 \pm 0.2
7a	28 \pm 3	50 \pm 6
7b	16 \pm 9	103 \pm 6
8a ^d	16 \pm 3	88 \pm 15
8b	7.6 \pm 1.9	187 \pm 5
9a	39 \pm 4	36 \pm 3
9b	16 \pm 7	98 \pm 4
10	44 \pm 6	32 \pm 5
11	99 \pm 5	14 \pm 1
12	107 \pm 12	13 \pm 1

^aResults are expressed as the mean \pm SD. ^b Cl_{int} = in vitro intrinsic clearance. ^c $t_{1/2}$ = in vitro half-life. ^d**8a** (2:1 ratio of **8a** and **8b**).

In the methylated series, analogues **2**, **3**, and **5** resulted in more stable compounds with low or moderate risk for high first pass metabolism and increased $t_{1/2}$ up to 50 times (cf. **1** with **2**). However, internal or C-terminal methylation of the nitrogen (**4** and **6**, respectively) did not improve the metabolic stability. In all the rigidified analogues the metabolic stability increased and the half-life became 4–16 times longer (cf. **1** with **7a–8b**). Furthermore, methylation at the β -carbon (compound **9a** and **9b**) or elongation of the phenylalanine (see compound **10**) also improved the metabolic stability, while decoration of the aromatic ring of the C-terminal phenylalanine did not influence the stability (cf. **1** with **11** and **12**).

In Vitro Permeability and Uptake Experiments. The intestinal epithelial permeability, expressed as apparent permeability coefficients (P_{app}), was determined from transport rates across Caco-2 cell monolayers, as described previously.²⁸ The experiments were run in both apical to basolateral (a–b) and basolateral to apical (b–a) directions (Table 3). In general a P_{app} value below 0.2×10^{-6} cm/s indicates low permeability, a P_{app} value ranging from 0.2×10^{-6} to 1.6×10^{-6} cm/s moderate permeability, and a P_{app} value above 1.6×10^{-6} cm/s indicates high permeability.²⁹ From Table 3 it is, however, clear that significant efflux occurs for most compounds, presumably by P-glycoprotein (PgP). However, despite the cell permeation in the absorptive a–b direction being obscured by the efflux, some compounds (**2**, **3**, **4**, **5**, **7a,b**, **8a,b**, and **9b**) show a moderate to high a–b rate of transport. This indicates that for these compounds the cell membrane and hence the cell monolayer permeability is high to very high.

Some of the compounds showed a very low recovery, i.e., poor mass balance, especially in the a–b direction (see Table 3). This is most likely due to high activity of apical brush-border peptidases. As seen in Table 3, there is a clear distinction in the mass balance of unstable compounds when comparing a–b and b–a. In the apical direction, the exposure to the peptidolytic enzymes is immediate, whereas the exposure is delayed when applying the compound initially on the basolateral side. Thus, for the unstable compounds, the calculations of the P_{app} values were corrected for the poor mass balance by mathematically adjusting the apparent donor concentration over the experimental time (the donor concentration degradation was simulated by a single

Table 3. Uptake and Permeability Data of Compounds 1–12^a

compd	uptake ^b			Caco-2 permeability			
	(pmol/mg protein)/min		ratio PEPT1/K1	P_{app} ^c (10^{-6} cm/s)		mass balance (%) (a-b)/(b-a)	ratio (b-a)/(a-b)
	CHO-PEPT1	CHO-K1		a-b ^d	b-a ^e		
1 ^f	0.3 ± 0.0	0.3 ± 0.0	1.0	0.12 ± 0.01	0.42 ± 0.03	3:33	3.6
2	2.2 ± 0.7	2.4 ± 0.5	0.9	13.9 ± 0.5	124 ± 21	77:85	8.9
3	1.1 ± 0.2	1.5 ± 0.2	0.7	18.4 ± 0.1	86.5 ± 0.2	76:82	4.7
4	18.8 ± 0.3	23.0 ± 2.5	0.8	9.0 ± 2.1	124 ± 19	90:86	14
5	32.7 ± 1.8	32.1 ± 8.6	1.0	20.4 ± 2.0	224 ± 5	93:121	11
6 ^f	0.3 ± 0.1	0.4 ± 0.1	0.7	2.2 ± 1.2	1.3 ± 0.3	0.5:56	0.6
7a	30.9 ± 4.1	22.3 ± 2.2	1.4	0.54 ± 0.02	26.3 ± 1.0	84:95	53
7b	14.9 ± 2.2	10.9 ± 1.2	1.4	0.76 ± 0.06	76.2 ± 1.1	90:95	95
8a ^g	13.1 ± 2.3	11.2 ± 1.30	1.2	3.6 ± 0.4	75.1 ± 2.1	81:109	21
8b	11.4 ± 1.0	8.7 ± 0.8	1.3	0.58 ± 0.03	51.4 ± 1.8	95:110	86
9a ^f	0.6 ± 0.1	0.7 ± 0.0	0.9	1.2 ± 0.1	5.8 ± 0.6	34:76	5.0
9b	24.8 ± 3.8	22.2 ± 3.1	1.1	4.4 ± 0.1	171 ± 6	93:123	39
10 ^f	0.6 ± 0.00	0.9 ± 0.15	0.7	0.19 ± 0.03	1.1 ± 0.3	13:74	5.8
11 ^f	0.8 ± 0.1	1.3 ± 0.3	0.6	0.58 ± 0.06	0.65 ± 0.10	1:56	1.1
12 ^f	0.2 ± 0.0	0.3 ± 0.0	0.7	1.5 ± 0.2	1.2 ± 0.2	1:54	0.8

^aResults are expressed as the mean ± SD. All compounds were analyzed at 100 μM. See Experimental Section for experimental conditions. ^bThe PEPT1 substrate [¹⁴C]GlySar was used as positive control. The use of the radioactive substrate allowed comparison with historical data and consistency of performance over time of PEPT1 activity in this cell line. The ratio PEPT1/K1 for [¹⁴C]GlySar was equal to or larger than 5 under the applied conditions. ^c P_{app} = apparent permeability coefficient. ^da-b = apical to basolateral. ^eb-a = basolateral to apical. ^f P_{app} corrected for poor mass balance using a single exponential decay function to account for compound degradation over the course of the experiment. ^g8a (2:1 ratio of 8a and 8b).

exponential decay function using the initial (c_0) concentration and the final (c_{final}) concentration).

The permeability data in the a-b direction showed that the methylated analogues 2–6 had high permeability (ranging from 2.2×10^{-6} to 20×10^{-6} cm/s). Thus, backbone methylation significantly increased the cell permeability in comparison to the reference compound H-Phe-Phe-NH₂ (1, 0.12×10^{-6} cm/s). The cyclized analogues 7a, 7b, and 8b together with compound 9a were classified as having moderate permeability (ranging from 0.5×10^{-6} to 1.2×10^{-6} cm/s) and the analogues 8a and 9b to have high permeability (3.6×10^{-6} and 4.4×10^{-6} cm/s, respectively). The C-terminal modified analogue with a one-carbon elongation in the side chain, compound 10 ($P_{app} = 0.19 \times 10^{-6}$ cm/s), showed similar low permeability as seen for compound 1. On the other hand, the methylated and the fluorinated C-terminal modified H-Phe-Phe-NH₂ analogues (11 and 12) were accompanied by a slight improvement in permeability compared to compound 1, with moderate P_{app} values of 0.58×10^{-6} and 1.5×10^{-6} cm/s, respectively. Moreover, compounds 11 and 12, together with compound 6, were the only analogues that did not show significant efflux. The rest of the compounds displayed a 5- to 95-fold higher transport rate in the b-a direction than in the a-b direction (Table 3).

Uptake studies with CHO-K1 and CHO-PEPT1 cells (control and PEPT1 stably transfected cells, respectively) were performed, and the results are expressed as (pmol/mg of protein)/min (Table 3). If the compounds are substrates for the peptide transporter PEPT1 and actively transported into the cell, the PEPT1/K1 ratio should be greater than 1. The PEPT1/K1 ratios for the synthesized compounds ranged from 0.6 (11) to 1.4 (7a and 7b), which indicates that these compounds are not actively transported. The rate of compound uptake into CHO cells is not directly comparable to compound permeability across the Caco-2 cell monolayers. However, a qualitative comparison is possible. Thus, in general, compounds

having a high uptake into CHO cells also have a higher permeability in Caco-2 cells.

Computational Analysis. The pharmacophore hypothesis generation program Phase³⁰ was used to investigate if the low-energy conformations of the high affinity ligands could position important structural features in common regions of space not accessible to the ligands with lower affinity. The dipeptides with K_i values of 10 nM or lower and known stereochemistry were defined as strong binders (1, 4, 10, and 12). No compounds in the series were devoid of affinity, but the three dipeptides with lowest affinity ($K_i = 70$ –190 nM) and known stereochemistry were defined as weak binders (2, 3, and 6). With the requirement that all four strong binders should match a derived pharmacophore hypothesis the maximum number of pharmacophore features was found to be 6 in order to obtain pharmacophore hypotheses. Further evaluation of these hypotheses identified two sets of pharmacophore features. One set resulting in 242 hypotheses consisted of two hydrogen bond acceptors, one donor, one positively charged group, and two aromatic rings. The other set was very similar with the difference that two hydrogen bond donors were included, of which one replaced the positively charged group. This set of pharmacophore features resulted in 2145 hypotheses. The hypotheses were scored by matching the strong binders to the pharmacophore hypotheses. With the default filter and complete clustering 39 hypotheses with scores of 3.42–3.65 remained after scoring. A final score for each hypothesis was derived by subtracting the matching scores of the weak binders from the score obtained when matching the strong binders, resulting in scores of 0.77–1.57. The 10 pharmacophore hypotheses with the highest final scores were visually inspected, and the compounds excluded from the set of strong binders were aligned to the hypotheses, with the requirement that they match all six pharmacophore features. The top ranked pharmacophore hypothesis represented a common binding pose for the strong binders that the weak binders had

difficulties attaining. Binding poses from alignment to the remaining pharmacophore hypotheses either could not explain the affinity of the rigidified analogues (e.g., neither **8a** nor **8b** could match the hypothesis, although one of them has the highest affinity in the series) or resulted in high fitness scores for some of the weak binders. The top ranked pharmacophore hypothesis is shown together with **1** in Figure 1, and the fitness

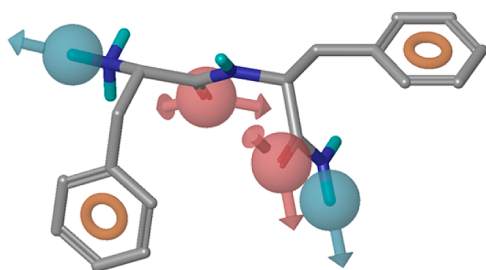


Figure 1. Binding pose of **1** derived from alignment to the top score pharmacophore hypothesis. The pharmacophore hypothesis features are orange torus = aromatic feature, blue sphere = hydrogen bond donor feature, and red sphere = hydrogen bond acceptor feature.

scores for the compounds attaining this pharmacophore hypothesis are presented in Table 4. In general the defined

Table 4. Fitness Score for the Alignment to the Top Pharmacophore Hypothesis for Compounds 1–12 and Their Set Membership in the Analysis

compd	fitness ^a	set ^b
1	3	SB
2	2.19	WB
3	1.7	WB
4	2.58	SB
5	2.27	NA
6	2.07	WB
7a	1.38	NA
7b	0.38	NA
8a	2.65	NA
8b	1.13	NA
9a	2.7	NA
9b	0.69	NA
10	2.14	SB
11	2.92	NA
12	2.96	SB

^aThe sum of the vector, site, and volume scores (range 0–3). ^bSB = strong binder, compounds used for generating pharmacophore hypotheses (correspond to actives in phase). WB = weak binders, compounds used for filtering out hypotheses that match the lowest affinity ligands (correspond to inactives in phase). NA = not assigned, compounds not used in the phase analysis.

strong binders in the series have the highest fitness scores. Only **10** ($K_i = 6.2$ nM) was not among the very top scored compounds. Compounds **5** and **11** were not included in the sets used to derive the common binding pose, since they are outside the limits for a set membership in this investigation. However, especially **11** may be considered as a strong binder with $K_i = 11.5$ nM and was also shown to be able to attain the binding pose with a fitness score of 2.92, as good as the strong binder set in the series. Although the top scoring pharmacophore hypothesis also suffered from a rather high fitness score for the weak binders **2** and **6**, their scores could be

rationalized. Both **2** and **6** could attain a binding pose that matched all but one pharmacophore feature in the pharmacophore hypothesis, resulting in a fairly low penalty to their scores. The third weak binder **3** had a significantly lower score than the strong binders and was considered to be correctly classified. A quantitative model validation was not performed, since all defined strong binders and weak binders were used to derive the binding pose model and the K_i values of the diastereomers **7–9** were not assigned within the pairs. However, on the basis of the qualitative analysis, we considered the model to be suitable for the SAR analysis and to support the assignment of K_i values within the pairs of diastereomers. Furthermore, since the model provides a rational binding mode for compounds with high affinity to the SP_{1–7} binding site, the model may also be used as a template in future virtual screening campaigns to search for novel ligands to this target.

DISCUSSION

A potential specific receptor for the N-terminal partial sequences of SP in mouse spinal cord was already discussed in the beginning of the 1980s,³¹ but it was not until 1990, when it was found that the binding was specific, saturable, and reversible, that the hypothesis of a specific SP_{1–7} receptor was proposed.¹⁶ During the 1990s the biological roles of the N-terminal fragment of SP were investigated by several groups.^{7,14,32,33} More recently the SARs of SP_{1–7} and other ligands (e.g., EM-2) have been investigated by our group, leading to the discovery of dipeptides with high affinity to the SP_{1–7} binding site and with interesting pharmacological properties such as antinociceptive effects in animal models of neuropathic pain.^{21,23,24}

In the present study we are addressing the challenging task of transforming these dipeptides into compounds with more druglike features. One way to achieve this is to introduce local constraints in the peptide backbone by incorporation of *N*-methylamino acids.³⁴ The advantage of incorporating a single methyl group is that it provides a balance between decreasing conformational entropy sufficient to change the binding affinity while still allowing sufficient conformational flexibility for the ligand to adopt the conformation required for molecular recognition to the target. Furthermore, the incorporation of a methyl group often provides metabolic stability because of resistance to proteolytic degradation.^{35,36}

In the dipeptide series presented herein we introduced a methyl group in each position along the backbone of the dipeptide H-Phe-Phe-NH₂. Highest influence on binding affinity is seen when substituting the N-terminal amine or the C-terminal amide with a methyl group (**2** and **6**, respectively), resulting in reduced binding affinities by 17–23 times. A possible explanation for this can be seen when looking at the proposed binding pose for the series (Figure 2). The binding

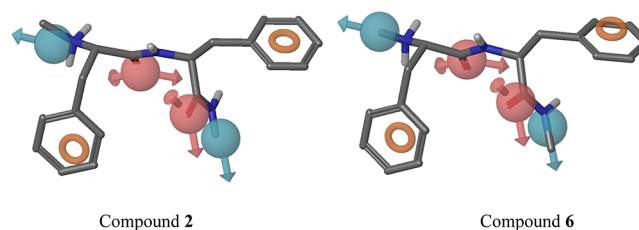


Figure 2. Binding poses of **2** and **6** when aligned to the top ranked pharmacophore hypothesis.

pose presented includes the spatial arrangement of six important interactions features that all high affinity compounds can present to the target protein, namely, two hydrogen bond acceptors, two hydrogen bond donors, and two aromatic rings. In **2** the methyl group on the N-terminus is positioned in the direction of the hydrogen bond donor vector from the amine to the protein in the pharmacophore hypothesis, suggesting a nonoptimal interaction in this part of the molecule with the target protein.

The hydrogen bond donor feature assigned to the amine would also be compatible with a positively charged feature in the series, and this was also found in other pharmacophore hypotheses. However, if that was the case, the directional property of the feature would be lost and compound **2** would have a higher fitness to the pharmacophore hypothesis. The reduced affinity observed for **6**, in which the primary amide was methylated to give a secondary amide, is also accounted for in the pharmacophore hypothesis because the hydrogen bond pattern for the C-terminal amide is optimal for a primary amide, which is present in all high affinity compounds in the series. This can be seen in Figure 2 where **6** is aligned to the pharmacophore, unable to match this hydrogen bond donor feature. When **1** was methylated on the internal nitrogen, no influence on the affinity potency could be observed (see compound **4**). The internal methylated dipeptide showed a tendency to ring-close to the corresponding diketopiperazine to some extent. Although the initial concentration of diketopiperazine was only ~10% in the test sample, further formation in the assay cannot be excluded, making the results hard to interpret in this case. However, internal methylation of the dipeptide, either in the opened or in the diketopiperazine form, seems to be allowed in terms of binding affinity.

To investigate the spatial arrangement of the phenylalanine side chains and the effect of more strongly rigidified H-Phe-Phe-NH₂ analogues, the compounds with side chain constraints **7** and **8** were synthesized. This modification was shown to display specific steric requirements as might be expected in a defined receptor pocket. When the *cis*-3-phenylpyrrolidine moiety was introduced at the N-terminal (**7a** and **7b**), the affinity dropped 4–6 times. Both these diastereomers show low fitness scores to the proposed pharmacophore, indicating that the compounds cannot adopt an optimal binding conformation. Interestingly, however, when the *cis*-3-phenylpyrrolidine moiety was incorporated in the C-terminal, the phenyl group seems to be well positioned in the active binding site in one of the diastereomers, resulting in almost 4 times higher binding affinity. From a comparison of **8a** and **8b** (Figure 3), a clear difference in fitness to the pharmacophore hypothesis is seen, supporting the (*S,S*)-configuration of the *cis*-3-phenylpyrrolidine in the high-affinity analogue **8a**.

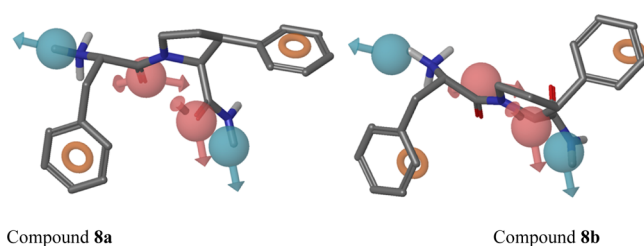


Figure 3. Binding poses of **8a** and **8b** when aligned to the pharmacophore hypothesis.

A β -methylation of the phenylalanine side chain can have an effect on how the side chain interacts with the binding site.³⁷ When a methyl group was introduced on the β -carbon in the C-terminal phenylalanine in **1**, a 4-fold difference between the (*S,S*)- and the (*R,R*)-configuration could be observed (cf. **9a** with **9b**). Inspecting the fitness scores of the two diastereomers when matched to the pharmacophore supports **9a** with the (*S,S*)-configuration of the β -methylphenylalanine as the analogue with highest binding affinity. Furthermore, a β -methylation reduces the conformational flexibility of the phenylalanine side chain by imposing a steric rotational constraint, which can be advantageous by reducing entropic penalty upon binding. However, this was not advantageous for the binding, since **1** possessed 2 times higher binding affinity compared to **9a**.

Elongation of the C-terminal phenylalanine side chain was well tolerated (cf. **1** with **10**), which indicates that there is room for modification in this part of the molecule. Interestingly, this is in contrast to the previous SAR investigation that resulted in identification of H-Phe-Phe-NH₂. Then the replacement of the C-terminal phenylalanine for a phenylglycine resulted in a completely inactive compound and even replacing the phenyl ring with thiophene resulted in significantly lower affinity.²³ Moreover, results herein suggest that the binding pocket seems to tolerate substituents on the aromatic moiety, since both compound **11** and compound **12** showed excellent binding affinities, especially compound **12** ($K_i = 3.3$ nM) in which a hydrogen in the meta position has been exchanged by a fluorine atom. This is somewhat contradictory to the result of the previous SAR investigation where the same C-terminal amino acids as in **11** and **12** in combination with O-methylated tyrosin and cyclohexylalanine as the N-terminal amino acids, respectively, were devoid of affinity to the SP₁₋₇ binding site. However, in the latter case the main problem might be that the change in both terminal parts was done concurrently, which gave a negative synergistic effect upon binding. Altogether, it seems that minor C-terminal changes are allowed if the N-terminal is preserved.

The in vitro pharmacokinetic properties of the compounds were also studied, i.e., active uptake via the dipeptide transporter PEPT1 in CHO cells, permeability and efflux in Caco-2 cells, and metabolic stability in human liver microsomes (Tables 2 and 3). The metabolic stability study was concentrated to the liver, since this organ constitutes the major site of metabolism for most drugs.²⁵ By use of the in vitro parameter intrinsic clearance (Cl_{int}), an estimate of the rate of liver metabolism (typically oxidative) of the compounds under in vivo conditions is obtained, which gives an indication of which compounds to select for further preclinical development.²⁶ Methyl groups incorporated into the peptide backbone can increase the metabolic stability. Indeed, the stability increased for all the methylated analogues of H-Phe-Phe-NH₂ except for the internal (**4**) and the C-terminal (**6**) N-methylated analogues. However, the apparent instability of the internal N-methylated compound is partly explained by the fact that the opened analogue to some extent might ring-close into the corresponding diketopiperazine form as mentioned earlier. To our satisfaction, the rigidified analogues of H-Phe-Phe-NH₂ resulted not only in metabolically more stable compounds (**7a–8b**) but also in the most potent binder **8a**. In fact, **8a** turned out to be 7 times more stable than H-Phe-Phe-NH₂, which makes this analogue a good candidate for replacing **1** in further animal studies. Modifications of the C-

terminal phenylalanine in the form of elongation as in compound **10** or β -methylation also improved the stability. However, *o*-methyl and *m*-fluoro substitutions on the aromatic part of the phenylalanine do not seem to have any effect on the metabolism compared to H-Phe-Phe-NH₂ (**1**) itself.

Furthermore, the intestinal membrane permeability and the transport mechanism of the analogues in this series were investigated. The dipeptide/tripeptide transporter PEPT1 is expressed in the intestine and ensures efficient absorption of small peptides from digestion of dietary proteins. PEPT1 is also important for absorption of a variety of peptidomimetic drugs, such as β -lactam antibiotics and prodrugs of nucleoside analogues, such as valaciclovir.^{38,39} In order to achieve efficient binding and activation of the transporter, some important structural features of dipeptides need to be fulfilled: (1) no substitution at the N-terminal amine, (2) a negatively charged C-terminus, (3) an amide carbonyl oxygen, and (4) the interaction of the N- and C-terminal amino acids side chain with a proposed hydrophobic pocket, preferably aromatic groups.^{40–42} Thus, an efficient transport with PEPT1 was not expected for the synthesized dipeptides described in this paper which all contain primary amides in the C-terminal. However, the aromaticity, the dipeptide character, and the fact that some dipeptides with C-terminal amides have been shown to be PEPT1 substrates motivated us to investigate if the dipeptides in this series could be actively transported over the membrane. In general, the uptake studies using CHO cells transfected with the transporter PEPT1 indicated that the compounds are not good substrates for this transport system (see PEPT1/K₁ ratio in Table 3, all around 1). A very weak increase of PEPT1 activation could be seen for the dipeptides incorporating the *cis*-3-phenylpyrrolidine moiety (**7a–8b**), and this might be explained by the study of Vig et al.⁴³ where they demonstrated that dipeptides with a proline at the C- or N-terminal with the proper attendant amino acid exhibits both high affinity and activation of the PEPT1 transporter.

Although the compounds were not actively transported, the permeability data in the a–b direction generally indicated that small modifications of a peptide can have a significant effect on cell permeability in Caco-2 cells, in particular backbone modifications (see Table 3). Thus, the lead compound H-Phe-Phe-NH₂ (**1**) has poor cell-permeability of 0.12×10^{-6} cm/s, whereas the backbone methylated compounds **2–6**, a proline-based analogue (**8a**), and a β -methylated compound (**9b**) are highly permeable compounds (P_{app} values of $(2.2–18) \times 10^{-6}$ cm/s). However, one should be aware that some of the peptide compounds also were degraded over the Caco-2 cell membrane, as reflected in poor mass balances. This was the case for the nonbackbone modified peptides **1**, **6**, **9a**, and **10–12**. The degradation is most probably a result of protease activity in the cell membrane in the apical region. It is well-known that brush border proteases are expressed in Caco-2 cells.^{44,45} The set of sensitive peptides, all with a normal peptide backbone, are well in line with the structural preference for proteases. A majority of the peptides with a low recovery were also accompanied by a high clearance in the human liver microsomes (Table 2), indicating also a contribution of protease mediated degradation here besides the normally dominating oxidative metabolism. To investigate this, we performed a separate experiment with HLM supplemented with or without NADPH (cofactor for CYP450) (Figure 4). From Figure 4 it is clear that both oxidative and proteolytic activity is important for the more unstable compound (**6**, (–))

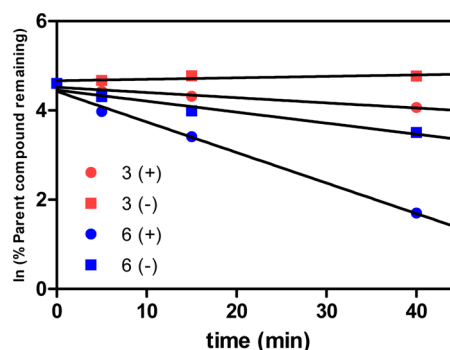


Figure 4. Metabolic stability of compounds **3** (red) and **6** (blue) in human liver microsomes with (+) and without (–) the CYP450 cofactor NADPH.

$t_{1/2} = 28$ min, (+) $t_{1/2} = 10$ min), and for the stable compound only oxidative metabolism contributes to the degradation (**3**, (–) $t_{1/2} =$ no metabolism detected, (+) $t_{1/2} = 60$ min).

Satisfyingly, compound **8a** with highest binding affinity ($K_i = 2.2$ nM) seems to possess both high stability ($Cl_{int} = 16 \mu\text{L min}^{-1} \text{mg}^{-1}$ and a high stability in Caco-2-cells) and high permeability (3.6×10^{-6} cm/s).

The efflux transporter PgP has an important role in limiting entry of various drugs into the central nervous system, which makes it an important factor to be considered when working with CNS active compounds.⁴⁶ PgP is also expressed in the human intestine, but its effect on limiting absorption of average dosed drugs is less pronounced than in the CNS. In drug discovery, an efflux ratio of 2 or larger is considered significant.⁴⁷ Several of the analogues studied in here displayed a large efflux (the ba/ab ratio ranging from 0.6 to 95), which might be explained by interactions with PgP. Nevertheless, in the Caco-2 cells other efflux transporters are also present and could be involved in the secretion of the compounds. To be noticed though is that the efflux was substantially lower for the methylated analogues (**2–6**) compared to the rigidified ones (**7a–8b**). Also, the stereochemistry seemed to influence the efflux, since there were big differences in the ba/ab ratios between all the diastereomers (cf. **7a** and **7b**, **8a** and **8b**, **9a** and **9b**).

CONCLUSION

Constrained and modified dipeptides analogues of H-Phe-Phe-NH₂ have been synthesized and evaluated regarding their binding affinity, uptake, permeability, and metabolic stability. In general, local constraints such as methylation of the peptide backbone or incorporation of pyrrolidines into the peptide backbone delivered compounds with increased metabolic stability and improved intestinal permeability. Unfortunately, the propensity for efflux was not reduced. C-Terminal rigidification of H-Phe-Phe-NH₂ using a *cis*-3-phenylpyrrolidine moiety with (*S,S*)-configuration (compound **8a**) was the only modification resulting in retained affinity to the SP_{1–7} binding site, besides improved stability and cell permeability. Moreover, in this study we have shown that it is possible to make changes in the C-terminal, e.g., substitution with *o*-methyl or *m*-fluoro in the aromatic part or elongation of the phenylalanine side chain without any loss in binding affinity. The results herein will be of significant value for further design of bioavailable research tools useful in forthcoming animal studies to clarify the physiological role of SP_{1–7} in pain of neuropathic origin.

EXPERIMENTAL SECTION

General Methods. Preparative RP-HPLC was performed on a system equipped with a Zorbax SB-C8 column (150 mm × 21.2 mm) or a 10 μ m Vydac C18 column (250 mm × 22 mm), in both cases with UV detection at 230 nm. Analytical RP-HPLC–MS was performed on a Gilson-Finnigan ThermoQuest AQA system (Onyx monolithic C18 column, 50 mm × 4.6 mm; MeCN/H₂O gradient with 0.05% HCOOH) in ESI mode, using UV (214 and 254 nm) and MS detection. The purity of each of the peptides was determined by RP-HPLC using the columns ACE 5 C18 (50 mm × 4.6 mm) and ACE 5 phenyl (50 mm × 4.6 mm) or Thermo Hypersil Fluophase RP (50 mm × 4.6 mm) with a H₂O/MeCN gradient with 0.1% TFA and UV detection at 220 nm. All peptides showed purity above 95%.

NMR spectra were recorded on a Varian Mercury plus spectrometer (¹H at 399.8 MHz and ¹³C at 100.5 MHz or ¹H at 399.9 MHz and ¹³C at 100.6 MHz) at ambient temperature. Chemical shifts (δ) are reported in ppm referenced indirectly to TMS via the solvent residual signal. Exact molecular masses were determined on a Micromass Q-ToF2 mass spectrometer equipped with an electrospray ion source at the Department of Pharmaceutical Biosciences, Uppsala University, Sweden. All other chemicals and solvents were of analytical grade from commercial sources.

General Synthesis of Peptides 1–12. *Coupling.* The peptides 1–12 were synthesized manually from Rink amide MBHA resin (0.66 mmol/g) or methylindole AM resin (0.63 mmol/g) in 2 mL disposable syringes fitted with porous polyethylene filter. Standard Fmoc conditions were used. The Fmoc protecting group was removed by treatment with 20% piperidine in DMF (2 × 1.5 mL, 2 + 10 min), and the polymer was washed with DMF (6 × 1.5 mL, 6 × 1 min). Coupling of the appropriate amino acid Fmoc-AA-OH (1.5 or 4 equiv) was performed in DMF (1.5 mL) using *N*-[(1*H*-benzotriazole-1-yl)-(dimethylamino)methylene]-*N*-methylmethanaminium hexafluorophosphate *N*-oxide (HBTU, 1.5 or 4 equiv) in the presence of DIEA (3 or 8 equiv). The resin was washed with DMF (5 × 1.5 mL, 5 × 1 min) and subsequently deprotected and washed as described above. After completion of the coupling cycle the resin was also washed with several portions of DMF, CH₂Cl₂, and MeOH before it was dried in a vacuum overnight.

Cleavage. The final peptide was cleaved from the resin by treatment with triethylsilane (100 μ L) and 95% aqueous trifluoroacetic acid (TFA, 1.5 mL) followed by agitation for 2 h at room temperature. The resin was filtered off and washed with TFA (2 × (0.3–0.5) mL). The filtrate was collected in a centrifuge tube and concentrated in a stream of nitrogen. Cold diethyl ether (\leq 7 mL) was used to precipitate the product, which was collected by centrifugation, washed with cold diethyl ether (\leq 3 × 7 mL), and dried.

Purification. The crude peptide was dissolved in MeCN/0.1% aqueous TFA, filtered through a 0.45 μ m nylon membrane, and purified in one to two runs by RP-HPLC. Selected fractions were analyzed by RP-HPLC and RP-HPLC–MS, and those containing pure product were pooled and lyophilized. The reported yields are based on the loading of the starting resin.

Peptide 1 (H-Phe-Phe-NH₂). The analogue was prepared according to the general procedure using Rink amide MBHA resin (313 mg, 200 μ mol), Fmoc-Phe-OH (310 mg, 800 μ mol), HBTU (303 mg, 800 μ mol), and DIEA (278 μ L, 1600 μ mol). Reaction time was 18 h. The crude peptide was purified by RP-HPLC to give **1** as a white solid in 23 mg (37% yield). HPLC purity: C18 column, >99%; Fluophase, >98%. Spectral data were in agreement with data from previous reports.²³

Peptide 2 (N-Me-Phe-Phe-NH₂). The analogue was prepared according to the general procedure using Rink amide MBHA resin (157 mg, 100 μ mol), Fmoc-Phe-OH (155 mg, 400 μ mol), Fmoc-N-Me-Phe-OH (161 mg, 400 μ mol), HATU (152 mg, 400 μ mol), and DIEA (139 μ L, 800 μ mol). Reaction time was 18 h. The crude peptide was purified by RP-HPLC to give **2** as a white solid in 14.8 mg (45% yield). HPLC purity: C18 column, >99%; Fluophase, >98%. ¹H NMR (CD₃OD) δ 2.11 (s, 3H), 2.79 (dd, *J* = 10.4, 13.9 Hz, 1H), 3.05–3.15 (m, 2H), 3.21 (dd, *J* = 5.0, 13.9 Hz, 1H), 3.86–3.93 (m, 1H), 4.77

(dd, *J* = 5.0, 10.4 Hz, 1H), 7.18–7.36 (m, 10H). ¹³C NMR (CD₃OD) δ 32.1, 37.9, 39.3, 55.5, 64.1, 127.9, 129.0, 129.5, 130.2, 130.5, 130.51, 135.0, 138.4, 167.7, 174.8. HRMS (*M* + *H*⁺): 326.1870, C₁₉H₂₃N₃O₂ requires 326.1869.

Peptide 3 (α -Me-Phe-Phe-NH₂). The analogue was prepared according to the general procedure using Rink amide MBHA resin (157 mg, 100 μ mol), Fmoc-Phe-OH (155 mg, 400 μ mol), Fmoc- α -Me-Phe-OH (161 mg, 400 μ mol), HATU (152 mg, 400 μ mol), and DIEA (139 μ L, 800 μ mol). Reaction time was 20 h. The crude peptide was purified by RP-HPLC to give **3** as a white solid in 3.6 mg (11.2% yield). HPLC purity: C18 column, >98%; Fluophase, >99%. ¹H NMR (CD₃OD) δ 1.38 (s, 3H), 2.98 (dd, *J* = 10.1, 13.9 Hz, 1H), 3.30 (d, *J* = 14.4 Hz, 1H), 3.23 (dd, *J* = 5.2, 13.9 Hz, 1H), 3.31 (d, *J* = 14.4 Hz, 1H), 4.78 (dd, *J* = 5.2, 10.1 Hz, 1H), 7.2–7.36 (m, 10H). ¹³C NMR (CD₃OD) δ 22.8, 39.2, 43.7, 55.7, 61.8, 127.9, 129.1, 129.5, 130.0, 130.4, 131.4, 134.2, 138.4, 171.5, 175.5. HRMS (*M* + *H*⁺): 326.1866, C₁₉H₂₃N₃O₂ requires 326.1869.

Peptide 4 (Phe-N-Me-Phe-NH₂). The analogue was prepared according to the general procedure using Rink amide MBHA resin (157 mg, 100 μ mol), Fmoc-N-Me-Phe-OH (161 mg, 400 μ mol), Fmoc-Phe-OH (155 mg, 400 μ mol), HATU (152 mg, 400 μ mol), and DIEA (139 μ L, 800 μ mol). Reaction time was 22 h. The crude peptide was purified with RP-HPLC and the pure fractions containing the dipeptide were collected, pooled, and lyophilized to give **4** as a white solid in 9.8 mg (30.1% yield). HPLC purity: C18 column, 94.6%; Fluophase, >92.1%. Subsequent NMR analysis of the product showed minor impurities. Thus, an analytical sample from the NMR solution was again analyzed by RP-HPLC and showed the product as a major peak along with two extra minor peaks. Repurification of the product was done using RP-HPLC. The major peak (corresponding to the dipeptide product) and the bigger of the two minor peaks were isolated and characterized by NMR and MS. The latter compound turned out to be the corresponding diketopiperazine (DKP). However, once again a minor portion of the pure isolated dipeptide converted into the DKP in the NMR solution. Thus, the formation of Phe-N-Me-Phe-NH₂ into some amount of the DKP seems to be unavoidable. ¹H NMR for **4** (CD₃OD) δ 2.82 (s, 3H), 2.95–3.15 (m, 4H), 4.51 (dd, *J* = 6.5, 7.6 Hz, 1H), 5.21 (dd, *J* = 7.4, 8.6 Hz, 1H), 7.13–7.39 (m, 10H). ¹³C NMR (CD₃OD) δ 32.69, 35.51, 37.98, 53.31, 60.31, 127.89, 129.03, 129.66, 130.09, 130.25, 130.59, 135.18, 138.41, 170.28, 173.66. HRMS (*M* + *H*⁺): 326.1866, C₁₉H₂₃N₃O₂ requires 326.1869.

¹H NMR for the corresponding diketopiperazine of **4** (CD₃OD) δ 1.41 (dd, *J* = 9.1, 13.5 Hz, 1H), 2.65 (dd, *J* = 3.8, 13.5 Hz, 1H), 2.78 (dd, *J* = 4.7, 14.2 Hz, 1H), 2.98 (s, 3H), 3.05 (dd, *J* = 4.7, 14.2 Hz, 1H), 3.98 (dd, *J* = 3.8, 9.1 Hz, 1H), 4.24 (t, *J* = 4.7 Hz, 1H), 6.95–7.03 (m, 2H), 7.15–7.41 (m, 8H). LC–MS: (*M* + *H*⁺) 309; (2*M* + *H*⁺) 617.

Peptide 5 (Phe- α -Me-Phe-NH₂). The analogue was prepared according to the general procedure using Rink amide MBHA resin (157 mg, 100 μ mol), Fmoc-Phe-OH (155 mg, 400 μ mol), Fmoc- α -Me-Phe-OH (161 mg, 400 μ mol), HATU (152 mg, 400 μ mol), and DIEA (139 μ L, 800 μ mol). Reaction time was 20 h. The crude peptide was purified by RP-HPLC to give **5** as a white solid in 17.3 mg (53.2% yield). HPLC purity: C18 column, >99%; Fluophase, >99%. ¹H NMR (CD₃OD) δ 1.46 (s, 3H), 2.97 (dd, *J* = 9.5, 14.2 Hz, 1H), 3.14 (dd, *J* = 5.6, 14.2 Hz, 1H), 3.25 (d, *J* = 13.4 Hz, 1H), 3.37 (d, *J* = 13.4 Hz, 1H), 4.10 (dd, *J* = 5.6, 9.5 Hz, 1H), 7.1–7.4 (m, 10H). ¹³C NMR (CD₃OD) δ 23.9, 38.6, 41.5, 55.9, 61.8, 127.99, 128.9, 129.2, 130.2, 130.4, 131.7, 135.9, 137.5, 168.9, 178.2. HRMS (*M* + *H*⁺): 326.1866, C₁₉H₂₃N₃O₂ requires 326.1869.

Peptide 6 (Phe-Phe-NHMe). The analogue was prepared according to the general procedure using indole AM resin (0.63 mmol/g) (159 mg, 100 μ mol), Fmoc-Phe-OH (155 mg, 400 μ mol), HATU (152 mg, 400 μ mol), and DIEA (139 μ L, 800 μ mol). Reaction time was 22 h. The crude peptide was purified by RP-HPLC to give **6** as a white solid in 25.7 mg (79.1% yield). HPLC purity: C18 column, >99%; Fluophase, >99%. ¹H NMR (CD₃OD) δ 2.65 (bs, 3H), 2.95 (dd, *J* = 7.6, 13.7 Hz, 1H), 3.03 (dd, *J* = 8.2, 14.2 Hz, 1H), 3.07 (dd, *J* = 7.4, 13.7 Hz, 1H), 3.23 (dd, *J* = 5.7, 14.2 Hz, 1H), 4.09 (dd, *J* = 5.7,

8.2 Hz, 1H), 4.55 (dd, $J = 7.4$, 7.6 Hz, 1H), 7.16–7.38 (m, 10H). ^{13}C NMR (CD_3OD) δ 26.2, 38.5, 39.2, 55.5, 56.6, 127.9, 128.8, 129.5, 130.1, 130.2, 130.5, 135.5, 138.1, 169.4, 173.1. HRMS ($\text{M} + \text{H}^+$): 326.1870, $\text{C}_{19}\text{H}_{23}\text{N}_3\text{O}_2$ requires 326.1869.

Peptides 7a and 7b (cis-3-Phenylpyrrolidine-Phe-NH₂). The analogues were prepared according to the general procedure using Rink amide MBHA resin (157 mg, 100 μmol), Fmoc-Phe-OH (155 mg, 400 μmol), racemic Fmoc-cis-3-phenylpyrrolidine-2-carboxylic acid (62 mg, 150 μmol), HBTU (152 mg, 400 μmol or 57 mg, 150 μmol), and DIEA (278 μL , 1600 μmol or 52 μL , 300 μmol). Reaction time was 24 h. The crude peptide mixture was purified, and the diastereomers were separated by RP-HPLC to give the pure diastereomers **7a** and **7b** as white solids in 5.4 mg (32% yield) and 9.3 mg (55%), respectively.

Peptide 7a. HPLC purity: C18 column, >99%; Fluophase, >99%. ^1H NMR (CD_3OD) δ 2.35–2.50 (m, 2H), 2.77 (dd, $J = 7.5$, 13.7 Hz, 1H), 3.00 (dd, $J = 6.5$, 13.7 Hz, 1H), 3.38 (m, $J = 7.4$, 9.7, 11.4 Hz, 1H), 3.73 (m, $J = 3.6$, 7.8, 11.4 Hz, 1H), 3.88 (ddm, $J = 7.4$, 9.3 Hz, 1H), 4.33 (dd, $J = 6.5$, 7.5 Hz, 1H), 4.48 (d, $J = 9.3$ Hz, 1H), 7.15–7.40 (m, 10H). ^{13}C NMR (CD_3OD) δ 31.63, 39.41, 46.62, 48.23, 55.53, 64.82, 127.82, 129.21, 129.41 (2C), 129.93, 130.34, 137.60, 137.99, 167.12, 173.84. HRMS ($\text{M} + \text{H}^+$): 338.1875, $\text{C}_{20}\text{H}_{23}\text{N}_3\text{O}_2$ requires 338.1869.

Peptide 7b. HPLC purity: C18 column, >99%; Fluophase, >99%. ^1H NMR (CD_3OD) δ 2.20 (dd, $J = 5.9$, 13.6 Hz, 1H), 2.41–2.49 (m, 2H), 2.50 (dd, $J = 8.6$, 13.6 Hz, 1H), 3.42 (ddm, $J = 8.7$, 11.2 Hz, 1H), 3.75 (dd, $J = 5.4$, 11.2 Hz, 1H), 3.89 (dm, $J = 8.8$ Hz, 1H), 4.11 (dd, $J = 5.9$, 8.6 Hz, 1H), 4.55 (d, $J = 9.3$ Hz, 1H), 6.94–6.99 (m, 2H), 7.16–7.36 (m, 8H). ^{13}C NMR (CD_3OD) δ 31.50, 38.58, 46.76, 48.38, 56.02, 64.65, 127.88, 129.19, 129.51, 129.64, 129.84, 130.18, 137.57, 137.70, 167.44, 178.22. HRMS ($\text{M} + \text{H}^+$): 338.1870, $\text{C}_{20}\text{H}_{23}\text{N}_3\text{O}_2$ requires 338.1869.

Peptides 8a and 8b (Phe-cis-3-phenylpyrrolidine-NH₂). The analogues were prepared according to the general procedure using Rink amide MBHA resin (157 mg, 100 μmol), racemic Fmoc-cis-3-phenylpyrrolidine-2-carboxylic acid (62 mg, 150 μmol), Fmoc-Phe-OH (155 mg, 400 μmol), HBTU (152 mg, 400 μmol or 57 mg, 150 μmol), and DIEA (278 μL , 1600 μmol or 52 μL , 300 μmol). Reaction time was 24 h. The crude peptide mixture was purified, and diastereomers were separated by RP-HPLC. Because of a difficult separation, diastereomer “8a” was isolated as white solid in 14.2 mg (42% yield) in a 2:1 ratio (**8a/8b**) and the pure diastereomer **8b** in 11.2 mg (33% yield). The synthesis and purification have been reproduced several times with the same outcome.

Peptide 8a. HPLC purity (2:1 ratio, **8a/8b**): C18 column, >99%; Fluophase, >99%. ^1H NMR for **8a** (CD_3OD) δ (2:1 ratio of **8a/8b**, major diastereomer reported) 2.18 (m, $J = 1.03$, 6.3, 12.3 Hz, 1H), 2.67 (m, $J = 8.6$, 10.6, 12.3 Hz, 1H), 3.04 (dd, $J = 7.7$, 14.4 Hz, 1H), 3.35 (dd, $J = 6.0$, 14.4 Hz, 1H), 3.59–3.74 (m, 3H), 4.38 (dd, $J = 6.0$, 7.7 Hz, 1H), 4.75 (d, $J = 8.7$ Hz, 1H), 7.11 (m, 1H), 7.21–7.53 (m, 9H). ^{13}C NMR (CD_3OD) δ (2:1 ratio of **8a/8b**, major diastereomer reported) 29.56, 38.30, 47.75, 47.95, 54.06, 65.61, 128.59, 129.17, 129.43, 129.44, 130.13, 130.71, 135.51, 137.49, 168.40, 174.46. HRMS ($\text{M} + \text{H}^+$): 338.1865, $\text{C}_{20}\text{H}_{23}\text{N}_3\text{O}_2$ requires 338.1869.

Peptide 8b. HPLC purity: C18 column, >99%; Fluophase, >99%. ^1H NMR (CD_3OD) δ 1.92 (m, $J = 1.2$, 6.2, 13.2 Hz, 1H), 2.58 (m, $J = 8.5$, 10.7, 11.8, 13.2 Hz, 1H), 2.73 (m, $J = 6.2$, 9.6, 10.9 Hz, 1H), 3.17 (d, $J = 7.6$ Hz, 2H), 3.31 (m, $J = 8.6$ Hz, 1H), 3.84 (m, $J = 1.2$, 8.5, 9.7 Hz, 1H), 4.42 (t, $J = 7.6$ Hz, 1H), 4.53 (d, $J = 8.6$ Hz, 1H), 7.11 (m, 1H), 7.21–7.45 (m, 10H). ^{13}C NMR (CD_3OD) δ 30.07, 37.70, 47.64, 47.72, 54.16, 65.54, 128.94, 129.25, 129.42, 129.49, 130.31, 130.85, 135.36, 137.79, 168.49, 173.78. HRMS ($\text{M} + \text{H}^+$): 338.1865, $\text{C}_{20}\text{H}_{23}\text{N}_3\text{O}_2$ requires 338.1869.

Peptides 9a and 9b (Phe- β -Me-Phe-NH₂). The analogues were prepared according to the general procedure using Rink amide MBHA resin (157 mg, 100 μmol), Fmoc-Phe-OH (155 mg, 400 μmol), (2R,3R)/(2S,3S)-racemic-Fmoc- β -methylphenylalanine (60 mg, 150 μmol), HBTU (152 mg, 400 μmol or 57 mg, 150 μmol), and DIEA (278 μL , 1600 μmol or 52 μL , 300 μmol). Reaction time was 24 h. The crude peptide mixture was purified and the diastereomers were

separated by RP-HPLC to give the pure diastereomers **9a** and **9b** as white solids in 4.7 mg (29% yield) and 4.5 mg (28% yield), respectively.

Peptide 9a. HPLC purity: C18 column, >98.4%; Fluophase, >97.8%. ^1H NMR (CD_3OD) δ 1.31 (dd, $J = 1.6$, 7.1 Hz, 3H), 2.95 (dd, $J = 8.4$, 14.3 Hz, 1H), 3.13–3.21 (m, 2H), 3.93 (ddd, $J = 1.6$, 5.0, 8.4 Hz, 1H), 4.65 (dd, $J = 1.6$, 9.7 Hz, 1H), 7.16–7.40 (m, 10H). ^{13}C NMR (CD_3OD) δ 19.9, 38.4, 42.9, 55.2, 59.6, 128.0, 128.8, 128.9, 129.6, 130.2, 130.5, 135.3, 144.0, 169.1, 175.2. HRMS ($\text{M} + \text{H}^+$): 326.1863, $\text{C}_{19}\text{H}_{23}\text{N}_3\text{O}_2$ requires 326.1869.

Peptide 9b. HPLC purity: C18 column, >99%; Fluophase, >99%. ^1H NMR (CD_3OD) δ 1.29 (dd, $J = 0.9$, 7.0 Hz, 3H), 2.42 (dd, $J = 8.9$, 14.5 Hz, 1H), 2.57 (dd, $J = 5.0$, 14.5 Hz, 1H), 3.13 (ddm, $J = 6.7$, 9.9 Hz, 1H), 3.95 (dd, $J = 5.0$, 8.9 Hz, 1H), 4.66 (dd, $J = 0.9$, 9.9 Hz, 1H), 6.96–7.01 (m, 2H), 7.17–7.33 (m, 8H). ^{13}C NMR (CD_3OD) δ 19.6, 38.3, 43.4, 55.4, 59.4, 128.1, 128.8, 128.9, 129.7, 130.1, 130.3, 135.3, 144.1, 169.1, 175.5. HRMS ($\text{M} + \text{H}^+$): 326.1868, $\text{C}_{19}\text{H}_{23}\text{N}_3\text{O}_2$ requires 326.1869.

Peptide 10 (Phe-homoPhe-NH₂). The analogue was prepared according to the general procedure using Rink amide MBHA resin (157 mg, 100 μmol), Fmoc-Phe-OH (155 mg, 400 μmol), Fmoc-homo-Phe-OH (161 mg, 400 μmol), HBTU (152 mg, 400 μmol), and DIEA (139 μL , 800 μmol). Reaction time was 18 h. The crude peptide was purified by RP-HPLC to give **10** as a white solid in 21.8 mg (67% yield). HPLC purity: C18 column, >99%; Fluophase, >99%. ^1H NMR (CD_3OD) δ 1.91–2.15 (m, 2H), 2.60–2.77 (m, 2H), 3.06 (dd, $J = 8.5$, 14.2 Hz, 1H), 3.31 (dd, $J = 5.9$, 14.3 Hz, 1H), 3.19 (dd, $J = 5.9$, 8.5 Hz, 1H), 4.41 (dd, $J = 5.4$, 8.5 Hz, 1H), 7.14–7.40 (m, 10H). ^{13}C NMR (CD_3OD) δ 33.0, 35.4, 38.6, 54.4, 55.6, 127.2, 128.9, 129.4, 129.5, 130.2, 130.6, 135.6, 142.4, 169.6, 175.8. HRMS ($\text{M} + \text{H}^+$): 326.1873, $\text{C}_{19}\text{H}_{23}\text{N}_3\text{O}_2$ requires 326.1869.

Peptide 11 (Phe-Phe(3-F)-NH₂). The analogue was prepared according to the general procedure using Rink amide MBHA resin (157 mg, 100 μmol), Fmoc-Phe-OH (155 mg, 400 μmol), Fmoc-3-Fluoro-Phe-OH (162 mg, 400 μmol), HBTU (152 mg, 400 μmol), and DIEA (139 μL , 800 μmol). Reaction time was 18 h. The crude peptide was purified by RP-HPLC to give **11** as a white solid in 12.9 mg (40% yield). HPLC purity: C18 column, 98.9%; Fluophase, 98.7%. ^1H NMR (CD_3OD) δ 2.98 (s, 3H), 3.00 (dd, $J = 7.6$, 14.0 Hz, 1H), 3.02 (dd, $J = 8.4$, 14.3 Hz, 1H), 3.12 (dd, $J = 7.6$, 14.0 Hz, 1H), 3.25 (dd, $J = 5.7$, 14.3 Hz, 1H), 4.09 (dd, $J = 5.7$, 8.4 Hz, 1H), 4.66 (dd, $J = 7.6$, 7.6 Hz, 1H), 7.07–7.21 (m, 4H), 7.26–7.41 (m, 5H). ^{13}C NMR (CD_3OD) δ 19.6, 36.5, 38.6, 54.7, 55.5, 127.0, 128.0, 128.9, 130.2, 130.5, 130.8, 131.4, 135.5, 136.1, 137.9, 169.3, 175.3. HRMS ($\text{M} + \text{H}^+$): 326.1866, $\text{C}_{19}\text{H}_{23}\text{N}_3\text{O}_2$ requires 326.1869.

Peptide 12 (Phe-Phe(2-Me)-NH₂). The analogue was prepared according to the general procedure using Rink amide MBHA resin (157 mg, 100 μmol), Fmoc-Phe-OH (155 mg, 400 μmol), Fmoc-2-methyl-Phe-OH (161 mg, 400 μmol), HBTU (152 mg, 400 μmol), and DIEA (139 μL , 800 μmol). Reaction time was 18 h. The crude peptide was purified by RP-HPLC to give **12** as a white solid in 12.4 mg (38% yield). HPLC purity: C18 column, >99%; Fluophase, >99%. ^1H NMR (CD_3OD) δ 2.98 (dd, $J = 8.4$, 13.9 Hz, 1H), 3.01 (dd, $J = 8.5$, 14.3 Hz, 1H), 3.15 (dd, $J = 6.3$, 13.9 Hz, 1H), 3.26 (dd, $J = 5.4$, 14.3 Hz, 1H), 4.08 (dd, $J = 5.4$, 8.5 Hz, 1H), 4.66 (dd, $J = 6.3$, 8.4 Hz, 1H), 6.92–7.00 (m, 1H), 7.01–7.13 (m, 2H), 7.26–7.40 (m, 6H). ^{13}C NMR (CD_3OD) δ 38.6, 38.7, 55.5, 55.7, 114.6 ($J = 21.4$ Hz), 117.0 ($J = 21.7$ Hz), 126.2 ($J = 2.77$ Hz), 128.9, 130.2, 130.5, 131.2 ($J = 8.29$ Hz), 135.4, 141.0 ($J = 7.56$ Hz), 164.3 ($J = 244.4$ Hz), 169.5, 174.9. HRMS ($\text{M} + \text{H}^+$): 330.1621, $\text{C}_{18}\text{H}_{20}\text{N}_3\text{O}_2\text{F}$ requires 330.1618.

[2,4-DehydroPro]SP₁₋₇. The precursor peptide for tritium-labeling [2,4-dehydroPro]SP₁₋₇ was prepared by standard solid-phase peptide synthesis techniques using Fmoc/*tert*-butyl protection and purified as described above. Tritium labeling of the precursor was performed by Amersham Biosciences (Cardiff, U.K.) and resulted in 370 MBq (10 mCi) of [^3H]SP₁₋₇ with a specific activity of 3.11 TBq/mmol (84 Ci/mmol).

Animal Experiment and Membrane Preparation. The preparations of receptor membranes were conducted using spinal cords from male Sprague–Dawley rats. The rats (Alab AB, Sollentuna,

Sweden), weighing 200–250 g, were housed in groups of four in air-conditioned rooms (22–23 °C and a humidity of 50–60%) under an artificial light–dark cycle and had free access to food and water. Prior to tissue sampling the rats were allowed to adapt to the laboratory environment for 1 week. The animals ($n = 15$) were killed by decapitation, and the spinal cords were rapidly removed and quickly frozen. Tissues were then kept at -80 °C until analyzed. The animal experiment was approved by the local ethical committee in Uppsala, Sweden.

The frozen spinal cords weighing approximately 250–300 mg/animal were thawed and placed on ice before being homogenized for 30 s in 30 volumes of ice-cold 50 mM Tris-HCl buffer (pH 7.4) containing 5 mM KCl and 120 mM NaCl, using a Polytron homogenizer. The homogenate was then centrifuged at 4000g for 20 min at 4 °C, and the supernatant was discarded. The resulting pellet was resuspended in 30 volumes of ice-cold 50 mM Tris-HCl buffer (pH 7.4) containing 300 mM KCl and 10 mM EDTA. Following incubation on ice for 30 min the sample was centrifuged at 4000g for 20 min at 4 °C. The pellet obtained was diluted and homogenized in 30 volumes of ice-cold 50 mM Tris-HCl containing 0.02% BSA, 5 mM EDTA, 3 mM MnCl_2 , and 40 μg bacitracin and recentrifuged twice as described above. The final pellet was resuspended and homogenized in 5 volumes of ice-cold 50 mM Tris-HCl buffer (pH 7.4) and immediately frozen at -80 °C until used in binding studies. The protein concentration of the membrane suspension was determined according to the method of Lowry⁴⁸ using bovine serum albumin as protein standard.

Radioligand Binding Assay. Assessment of the binding affinity for the various compounds analyzed in this study was carried out using the analogue [^3H]SP_{1–7} as tracer. Assays were performed in tubes containing 50 μL of spinal cord membrane suspension (200 μg of protein) and 0.9 nM [^3H]SP_{1–7} (specific activity, 3.11 TBq/mmol (84 Ci/mmol)) in a final volume of 0.5 mL of 50 mM Tris binding buffer (pH 7.4) containing, 3 mM MnCl_2 , 0.2% BSA, and peptidase inhibitors (40 $\mu\text{g}/\text{mL}$ bacitracin, 4 $\mu\text{g}/\text{mL}$ leupeptin, 2 $\mu\text{g}/\text{mL}$ aprotinin, and 4 $\mu\text{g}/\text{mL}$ phosphoramidon). The amounts of total and unspecific binding in percent of the total radioactivity added were approximately 7% and 1.7%, respectively. The competition experiments were determined at six different concentrations varying between 0.01 nM and 1 μM unlabeled compounds. Nonspecific binding was determined in the presence of 1 μM SP_{1–7}. Samples were incubated for 60 min at 4 °C before being terminated by rapid filtration under vacuum with a Brandel 24-sample cell harvester through Whatman GF/C glass fiber filters treated with a solution containing 50 mM Tris (pH 7.4), 0.3% polyethylenimine (PEI), and 0.5% Triton X-100 at 4 °C overnight. Filters were washed twice with 3 mL of cold 50 mM Tris-HCl (pH 7.4) complemented with 0.1 mg/mL BSA and 3 mM MnCl_2 . The filters were air-dried for about 60 min before the bound radioactivity was determined using a liquid scintillation counter (Beckman LS 6000IC) at 63% efficiency in 5 mL of counting scintillant. The specific binding was determined as the difference between total and unspecific binding. All assays were run at six concentrations in triplicate, and each assay was repeated at least three times at different days except for compound **8a**, which was tested at six concentrations in triplicate on the same day. The binding curve for **8a** is shown in Figure 5. Data and statistics from the competition experiments were analyzed in the GraFit program (Erithacus Software, U.K.).

Computational Analysis. Compounds 1–12 were built in Maestro⁴⁹ and imported to Phase.³⁰ The structures were ionized at pH 7.0 (i.e., protonation of the N-terminus). Conformations were generated in Phase using MacroModel with 200 search steps per rotatable bond of mixed MCMM/LMOD with sampling set to Thorough. Energy minimization was performed using maximum 100 steps of truncated Newton conjugate gradient minimization with convergence criterion set to 0.05 kJ mol⁻¹ Å⁻¹. The force field OPLS 2005⁵⁰ and the generalized-Born/surface area (GB/SA) model for water⁵¹ as solvation model were used. Conformations within 5 kcal mol⁻¹ of the lowest found energy minimum were saved, and redundant conformations were removed based on maximum atom

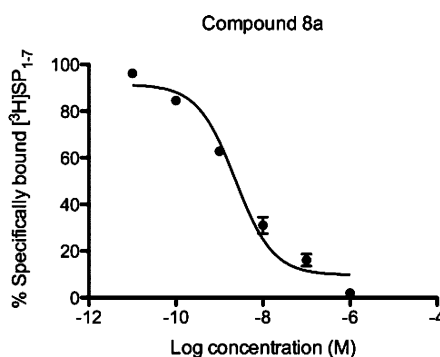


Figure 5. Inhibition of [^3H]SP_{1–7} binding by compound **8a**.

pair distance of 0.5 Å after superposition. The pharmacophore features found and assigned in the active compounds were hydrogen bond acceptors and donors, aromatic rings, and positively charged groups. The score formula used for pharmacophore hypothesis scoring was the sum of the vector, site, and volume scores plus a score for rewarding a high number of matches. Because the number of actives matching the pharmacophore hypotheses was 4 in all cases, the last term was set to a constant 1. The other terms in the formula have the range 0–1, which gives a matching score range of 1–4.

Metabolic Stability. Compounds (1 μM) were preincubated for 5 min at 37 °C with pooled human liver microsomes (0.5 mg/mL; Xenotech, KS) in 0.1 M potassium phosphate buffer, pH 7.4, prior to the addition of NADPH (1 mM) to initiate the reaction. Mixtures were then incubated for 0, 5, 15, and 40 min, and at each time point the reaction was stopped by the addition of acetonitrile (50% v/v). Plates were centrifuged at 3500 rpm for 20 min at 4 °C, and the supernatants were subjected to liquid chromatography/mass spectrometry analysis. The natural logarithm of the analytical peak area ratio (relative to 0 min sample which was considered as 100%) was plotted against time and analyzed by linear regression. In vitro half-life ($t_{1/2}$) and in vitro intrinsic clearance (Cl_{int}) were calculated on the basis of first-order reaction kinetics of the percentage of remaining compound. Dextromethorphan (3 μM) and midazolam (5 μM) were used as positive controls for cytochrome P450 enzymes (CYP) isoforms CYP2D6 and CYP3A4, respectively.

Cell Culture. Caco-2 cells (obtained from American Tissue Collection, Rockville, MD) were maintained in an atmosphere of 90% air and 10% CO_2 as described previously.²⁸ For transport experiments, 3.0×10^5 cells (passages 98–102) were seeded on polycarbonate filter inserts (12 mm diameter, pore size 0.4 μm ; Costar, Cambridge, MA) and allowed to grow and differentiate for 21–24 days. The integrity of the monolayers was assessed by measuring the paracellular marker [^{14}C]mannitol (1.0 $\mu\text{Ci}/\text{mL}$, 57.3 mCi/mmol; Perkin-Elmer Life Sciences, Boston, MA) transport and the trans-epithelial electrical resistance (TEER) before and after the experiments.

CHO-K1 and CHO-PEPT1 cells (control and stably transfected cells, respectively, were kind gifts from Dr. Anna-Lena Ungell, AstraZeneca Mölndal, Sweden) were maintained at 37 °C in an atmosphere of 90% air and 10% CO_2 , with DMEM containing 4.5 g/L glucose, 10% fetal bovine serum, 1% nonessential amino acids, and 50 $\mu\text{g}/\text{mL}$ gentamicin sulfate (Invitrogen, Carlsbad, CA). For the uptake experiments, 1.0×10^5 cells/well were seeded in 24-well plates and allowed to grow in antibiotic-free medium for 2 days.

Transcellular Transport and Uptake Experiments. Stock solutions (10 mM) of the peptides were prepared in dimethylsulfoxide (DMSO) and diluted to 100 μM (final DMSO concentration of 1%) in Hank's balanced salt solution (HBSS) containing 10 mM MES at pH 6.0 (HBSS pH 6.0) or containing 10 mM HEPES at pH 7.4 (HBSS pH 7.4). In all experiments, [^{14}C]glycylsarcosine ([^{14}C]GlySar, 1.82 μM , 0.1 $\mu\text{Ci}/\text{mL}$, 55 mCi/mmol; ARC, St. Louis, MO) was used as a PEPT1 substrate control. For inhibition controls, an excess of unlabeled competitor (10 mM; Sigma-Aldrich, St. Louis, MO) was used.

The intestinal epithelial permeability was determined from transport rates across Caco-2 cell monolayers. The cell monolayers were gently rinsed with HBSS, pH 6.0, and left to equilibrate in the same solution for 30 min at 37 °C. The transport experiments were run for 2 h at 37 °C and were started by the application of the compound solution to the donor side, which was the apical chamber in the apical to basolateral (a–b) experiments and the basolateral chamber in the basolateral to apical (b–a) experiments. Filter inserts were continuously stirred at 500 rpm on IKA-Schüttler MTS4 to obtain data that were unbiased by the aqueous boundary layer. The receiver chambers were sampled in suitable time points, and the samples were replaced with equal volumes of preheated receiver solution.

For transport studies performed under sink conditions, where less than 10% of the compound was transported across the Caco-2 cell monolayers, the apparent permeability coefficients (P_{app}) were calculated from the equation

$$P_{app} = \frac{\Delta Q}{\Delta t} \frac{1}{AC_0}$$

where $\Delta Q/\Delta t$ is the steady-state flux (mol/s), C_0 is the initial concentration in the donor chamber at each time interval (mol/mL), and A is the surface area of the filter (cm²). If the fraction transported exceeded 10%, the P_{app} coefficients were calculated applying nonsink conditions from the equation

$$C_R(t) = \frac{M}{V_D + V_R} + \left(C_{R0} - \frac{M}{V_D + V_R} \right) e^{-P_{app}A(1/V_D + 1/V_R)t}$$

where $C_R(t)$ is the time-dependent drug concentration in the receiver compartment (μ M), M is the amount of drug in the system (nmol), V_D and V_R are the volumes of the donor and receiver compartment (mL), respectively, and t is the time that has elapsed from the start of the interval (s).⁵² P_{app} was obtained from nonlinear regression of the accumulated dose in the receiver compartment over time, minimizing the sum of squared residuals in the equation.

Uptake studies with CHO cells were performed at 37 °C in HBSS, pH 6.0. Initially, cells were gently rinsed and left to equilibrate for 30 min at 37 °C. After the equilibration period, buffer was removed and replaced by compound diluted in HBSS, pH 6.0, and cells were incubated for 15 min at 37 °C. Uptake was terminated by buffer removal followed by two washes with ice-cold phosphate buffer saline (PBS). Cells were then lysed with acetonitrile/water (60:40, v/v) and centrifuged at 3500 rpm and 4 °C for 20 min. In the case of experiments with [¹⁴C]GlySar, 1 M sodium hydroxide solution was used for cell lysis. The results were expressed as (pmol/mg of protein)/min.

Data Analysis. Caco-2 and CHO cell permeability experiments were performed in, at least, triplicate and metabolic stability experiments in duplicate, and all samples were analyzed with liquid chromatography/mass spectrometry analysis on a ThermoFinnigan TSQ Quantum Discovery triple-quadrupole instrument (electrospray ionization, ESI; Thermo Electron Corp. Waltham, MA, U.S.) coupled to an Acquity ultrahigh performance LC system (Waters, Milford, MA). For chromatographic separation, an Acquity UPLC C18 column (1.7 μ m; Waters, Milford, MA) and a flow rate of 600 μ L/min were used. During the analysis an amount of 10 μ L of the samples was injected with a gradient with 0.1% formic acid in acetonitrile and 0.1% formic acid in water. Electrospray ionization was used in positive mode, and the daughter ions of m/z 120.1 (1, 6, and 12), 134.1 (2, 3, 4, 5, 9, and 11), 146.1 (7 and 8), and 281.2 (10) were used for quantification of the respective compounds. The internal standard warfarin (50 nM) was used throughout the analysis.

Radioactive samples ([¹⁴C]GlySar and [¹⁴C]mannitol) were analyzed with a liquid scintillation counter (TopCount NXT, Perkin-Elmer Life Sciences, Boston, MA). Cellular protein content was determined using a protein assay kit with bovine serum albumin (BSA) as standard (Thermo Scientific, Rockford, IL).

AUTHOR INFORMATION

Corresponding Author

*Phone: +46-18-4714285. Fax: +46-18-4714474. E-mail: Anja.Sandstrom@orgfarm.uu.se.

Author Contributions

The manuscript was written through contributions of all authors. All authors have given approval to the final version of the manuscript.

Notes

The authors declare no competing financial interest.

ACKNOWLEDGMENTS

We thank Dr. Milad Botros for technical assistance regarding the radioligand binding assay and Rebecka Strand for synthetic assistance. This work was supported by grants from the Swedish Research Council (Grants 9478 and 21386 and a grant to the Chemical Biology Consortium Sweden), Uppsala Berzelii Technology Centre for Neurodiagnostics, and the Knut and Alice Wallenberg Foundation. J.M.K. thanks CAPES/MEC/Brazil for his research fellowship.

ABBREVIATIONS USED

SP, substance P; NK-1, neurokinin-1; SAR, structure–activity relationship; EM-2, endomorphin-2; E1, endomorphin-1; PEPT1, dipeptide/tripeptide transporter; HLM, human liver microsome; Cl_{int} , intrinsic clearance; P_{app} , apparent permeability coefficient; $t_{1/2}$, in vitro half-life; DMSO, dimethylsulfoxide; HBSS, Hank's balanced salt solution

REFERENCES

- (1) Von Euler, U. S.; Gaddum, J. H. An unidentified depressor substance in certain tissue extracts. *J. Physiol.* **1931**, *72*, 74–87.
- (2) Nakanishi, S. Mammalian tachykinin receptors. *Annu. Rev. Neurosci.* **1991**, *14*, 123–136.
- (3) Hökfelt, T.; Pernow, B.; Wahren, J. Substance P: a pioneer amongst neuropeptides. *J. Intern. Med.* **2001**, *249*, 27–40.
- (4) Lee, C.-M.; Sandberg, B. E. B.; Hanley, M. R.; Iversen, L. L. Purification and characterization of a membrane-bound substance P-degrading enzyme from human brain. *Eur. J. Biochem.* **1981**, *114*, 315–327.
- (5) Sakurada, T.; Le Greves, P.; Stewart, J.; Terenius, L. Measurement of substance P metabolites in rat CNS. *J. Neurochem.* **1985**, *44*, 718–722.
- (6) Hallberg, M.; Nyberg, F. Neuropeptide conversion to bioactive fragments—an important pathway in neuromodulation. *Curr. Protein Pept. Sci.* **2003**, *4*, 31–44.
- (7) Kreeger, J. S.; Larson, A. A. Substance P-(1–7), a substance P metabolite, inhibits withdrawal jumping in morphine-dependent mice. *Eur. J. Pharmacol.* **1993**, *238*, 111–115.
- (8) Zhou, Q.; Carlsson, A.; Botros, M.; Fransson, R.; Sandström, A.; Gordh, T.; Hallberg, M.; Nyberg, F. The C-terminal amidated analogue of the substance P (SP) fragment SP_{1–7} attenuates the expression of naloxone-precipitated withdrawal in morphine dependent rats. *Peptides* **2009**, *30*, 2418–2422.
- (9) Zhou, Q.; Frändberg, P.-A.; Kindlundh, A. M. S.; Le Greves, P.; Nyberg, F. Substance P(1–7) affects the expression of dopamine D2 receptor mRNA in male rat brain during morphine withdrawal. *Peptides* **2003**, *24*, 147–153.
- (10) Wikteli, D.; Khalil, Z.; Nyberg, F. Modulation of peripheral inflammation by the substance P N-terminal metabolite substance P1–7. *Peptides* **2006**, *27*, 1490–1497.
- (11) Sakurada, C.; Watanabe, C.; Sakurada, T. Occurrence of substance P(1–7) in the metabolism of substance P and its antinociceptive activity at the mouse spinal cord level. *Methods Find. Exp. Clin. Pharmacol.* **2004**, *26*, 171–176.

- (12) Carlsson, A.; Ohsawa, M.; Hallberg, M.; Nyberg, F.; Kamei, J. Substance P1-7 induces antihyperalgesia in diabetic mice through a mechanism involving the naloxone-sensitive sigma receptors. *Eur. J. Pharmacol.* **2010**, *626*, 250–255.
- (13) Dyck, P. J.; Dyck, P. J. B.; Velosa, J. A.; Larson, T. S.; O'Brien, P. C.; Grp, N. G. F. S. Patterns of quantitative sensation testing of hypoesthesia and hyperalgesia are predictive of diabetic polyneuropathy. A study of three cohorts. *Diabetes Care* **2000**, *23*, 510–517.
- (14) Skilling, S. R.; Smullin, D. H.; Larson, A. A. Differential-effects of C-terminal and N-terminal substance-P metabolites on the release of amino-acid neurotransmitters from the spinal-cord. Potential role in nociception. *J. Neurosci.* **1990**, *10*, 1309–1318.
- (15) Mousseau, D. D.; Sun, X. F.; Larson, A. A. Identification of a novel receptor mediating substance-P-induced behavior in the mouse. *Eur. J. Pharmacol.* **1992**, *217*, 197–201.
- (16) Igwe, O. J.; Kim, D. C.; Seybold, V. S.; Larson, A. A. Specific binding of substance P aminoterminal heptapeptide [SP(1-7)] to mouse brain and spinal cord membranes. *J. Neurosci.* **1990**, *10*, 3653–3663.
- (17) Botros, M.; Hallberg, M.; Johansson, T.; Zhou, Q.; Lindeberg, G.; Frändberg, P.-A.; Toemboely, C.; Toth, G.; Le Greves, P.; Nyberg, F. Endomorphin-1 and endomorphin-2 differentially interact with specific binding sites for substance P (SP) aminoterminal SP1-7 in the rat spinal cord. *Peptides* **2006**, *27*, 753–759.
- (18) Botros, M.; Johansson, T.; Zhou, Q.; Lindeberg, G.; Tomboly, C.; Toth, G.; Le Greves, P.; Nyberg, F.; Hallberg, M. Endomorphins interact with the substance P (SP) aminoterminal SP1-7 binding in the ventral tegmental area of the rat brain. *Peptides* **2008**, *29*, 1820–1824.
- (19) Rimón, R.; Legreves, P.; Nyberg, F.; Heikkilä, L.; Salmela, L.; Terenius, L. Elevation of substance P-like peptides in the CSF of psychiatric-patients. *Biol. Psychiatry* **1984**, *19*, 509–516.
- (20) Nyberg, F.; Le Greves, P.; Sundqvist, C.; Terenius, L. Characterization of substance P(1-7) and (1-8) generating enzyme in human cerebrospinal fluid. *Biochem. Biophys. Res. Commun.* **1984**, *125*, 244–250.
- (21) Fransson, R.; Botros, M.; Nyberg, F.; Lindeberg, G.; Sandström, A.; Hallberg, M. Small peptides mimicking substance P (1-7) and encompassing a C-terminal amide functionality. *Neuropeptides* **2008**, *42*, 31–37.
- (22) Ohsawa, M.; Carlsson, A.; Asato, M.; Koizumi, T.; Nakanishi, Y.; Fransson, R.; Sandström, A.; Hallberg, M.; Nyberg, F.; Kamei, J. The effect of substance P₁₋₇ amide on nociceptive threshold in diabetic mice. *Peptides* **2011**, *32*, 93–98.
- (23) Fransson, R.; Botros, M.; Sköld, C.; Nyberg, F.; Lindeberg, G.; Hallberg, M.; Sandström, A. Discovery of dipeptides with high affinity to the specific binding site for substance P1-7. *J. Med. Chem.* **2010**, *53*, 2383–2389.
- (24) Ohsawa, M.; Carlsson, A.; Asato, M.; Koizumi, T.; Nakanishi, Y.; Fransson, R.; Sandström, A.; Hallberg, M.; Nyberg, F.; Kamei, J. The dipeptide Phe-Phe amide attenuates signs of hyperalgesia, allodynia and nociception in diabetic mice using a mechanism involving the sigma receptor system. *Mol. Pain* **2011**, *7* (85), 1–12.
- (25) Houston, J. B. Utility of in-vitro drug-metabolism data in predicting in-vivo metabolic-clearance. *Biochem. Pharmacol.* **1994**, *47*, 1469–1479.
- (26) Obach, R. S. Prediction of human clearance of twenty-nine drugs from hepatic microsomal intrinsic clearance data: an examination of in vitro half-life approach and nonspecific binding to microsomes. *Drug Metab. Dispos.* **1999**, *27*, 1350–1359.
- (27) Baranczewski, P.; Stanczak, A.; Sundberg, K.; Svensson, R.; Wallin, A.; Jansson, J.; Garberg, P.; Postlind, H. Introduction to in vitro estimation of metabolic stability and drug interactions of new chemical entities in drug discovery and development. *Pharmacol. Rep.* **2006**, *58*, 453–472.
- (28) Hubatsch, I.; Ragnarsson, E. G. E.; Artursson, P. Determination of drug permeability and prediction of drug absorption in Caco-2 monolayers. *Nat. Protoc.* **2007**, *2*, 2111–2119.
- (29) Bergström, C. A. S.; Strafford, M.; Lazorova, L.; Avdeef, A.; Luthman, K.; Artursson, P. Absorption classification of oral drugs based on molecular surface properties. *J. Med. Chem.* **2003**, *46*, 558–570.
- (30) *Phase*, version 3.1; Schrödinger, LLC: New York, NY, 2009.
- (31) Piercey, M. F.; Dobry, P. J. K.; Einspahr, F. J.; Schroeder, L. A.; Masiques, N. Use of substance-P fragments to differentiate substance-P receptors of different tissues. *Regul. Pept.* **1982**, *3*, 337–349.
- (32) Huston, J. P.; Hasenoehrl, R. U.; Boix, F.; Gerhardt, P.; Schwarting, R. K. W. Sequence-specific effects of neurokinin substance P on memory, reinforcement, and brain dopamine activity. *Psychopharmacology* **1993**, *112*, 147–162.
- (33) Tomaz, C.; Silva, A. C.; Nogueira, P. J. Long-lasting mnemotropic effect of substance P and its N-terminal fragment (SP1-7) on avoidance learning. *Braz. J. Med. Biol. Res.* **1997**, *30*, 231–233.
- (34) Rizo, J.; Gierasch, L. M. Constrained peptides: models of bioactive peptides and protein substructures. *Annu. Rev. Biochem.* **1992**, *61*, 387–418.
- (35) Turk, J.; Panse, G. T.; Marshall, G. R. alpha-Methyl amino acids. Resolution and amino protection. *J. Org. Chem.* **1975**, *40*, 953–955.
- (36) Boyle, S.; Guard, S.; Higginbottom, M.; Horwell, D. C.; Howson, W.; McKnight, A.; Martin, K.; Pritchard, M. C.; O'Toole, J.; et al. Rational design of high affinity tachykinin NK1 receptor antagonists. *Bioorg. Med. Chem.* **1994**, *2*, 357–370.
- (37) Haskell-Luevano, C.; Toth, K.; Boteju, L.; Job, C.; Castrucci, A. M. D.; Hadley, M. E.; Hruby, V. J. beta-Methylation of the Phe(7) and Trp(9) melanotropin side chain pharmacophores affects ligand–receptor interactions and prolonged biological activity. *J. Med. Chem.* **1997**, *40*, 2740–2749.
- (38) Brandsch, M. Transport of drugs by proton-coupled peptide transporters: pearls and pitfalls. *Expert Opin. Drug Metab.* **2009**, *5*, 887–905.
- (39) Brodin, B.; Nielsen, C. U.; Steffansen, B.; Frokjaer, S. Transport of peptidomimetic drugs by the intestinal di/tri-peptide transporter, PepT1. *Pharmacol. Toxicol.* **2002**, *90*, 285–296.
- (40) Bailey, P. D.; Boyd, C. A. R.; Bronk, J. R.; Collier, I. D.; Meredith, D.; Morgan, K. M.; Temple, C. S. How to make drugs orally active: a substrate template for peptide transporter PepT1. *Angew. Chem., Int. Ed.* **2000**, *39*, 505–508.
- (41) Rubio-Aliaga, I.; Daniel, H. Mammalian peptide transporters as targets for drug delivery. *Trends Pharmacol. Sci.* **2002**, *23*, 434–440.
- (42) Våbenö, J.; Lejon, T.; Nielsen, C. U.; Steffansen, B.; Chen, W. Q.; Hui, O. Y.; Borchardt, R. T.; Luthman, K. Phe-Gly dipeptidomimetics designed for the di-/tripeptide transporters PEPT1 and PEPT2: synthesis and biological investigations. *J. Med. Chem.* **2004**, *47*, 1060–1069.
- (43) Vig, B. S.; Stouch, T. R.; Timoszyk, J. K.; Quan, Y.; Wall, D. A.; Smith, R. L.; Faria, T. N. Human PEPT1 pharmacophore distinguishes between dipeptide transport and binding. *J. Med. Chem.* **2006**, *49*, 3636–3644.
- (44) Gupta, D.; Gupta, S. V.; Lee, K. D.; Amidon, G. L. Chemical and enzymatic stability of amino acid prodrugs containing methoxy, ethoxy and propylene glycol linkers. *Mol. Pharmaceutics* **2009**, *6*, 1604–1611.
- (45) Tehler, U.; Nelson, C. H.; Peterson, L. W.; Provoda, C. J.; Hilfinger, J. M.; Lee, K. D.; McKenna, C. E.; Amidon, G. L. Puromycin-sensitive aminopeptidase: an antiviral prodrug activating enzyme. *Antiviral Res.* **2010**, *85*, 482–489.
- (46) Giacomini, K. M.; Huang, S. M.; Tweedie, D. J.; Benet, L. Z.; Brouwer, K. L. R.; Chu, X. Y.; Dahlin, A.; Evers, R.; Fischer, V.; Hillgren, K. M.; Hoffmaster, K. A.; Ishikawa, T.; Keppler, D.; Kim, R. B.; Lee, C. A.; Niemi, M.; Polli, J. W.; Sugiyama, Y.; Swaan, P. W.; Ware, J. A.; Wright, S. H.; Yee, S. W.; Zamek-Gliszczynski, M. J.; Zhang, L. Membrane transporters in drug development. *Nat. Rev. Drug Discovery* **2010**, *9*, 215–236.
- (47) Polli, J. W.; Wring, S. A.; Humphreys, J. E.; Huang, L. Y.; Morgan, J. B.; Webster, L. O.; Serabjit-Singh, C. S. Rational use of in vitro P-glycoprotein assays in drug discovery. *J. Pharmacol. Exp. Ther.* **2001**, *299*, 620–628.

- (48) Lowry, O. H.; Rosebrough, N. J.; Farr, A. L.; Randall, R. J. Protein measurement with the Folin phenol reagent. *J. Biol. Chem.* **1951**, *193*, 265–275.
- (49) *Maestro*, version 9.0; Schrödinger, LLC: New York, NY, 2009.
- (50) Kaminski, G. A.; Friesner, R. A.; Tirado-Rives, J.; Jorgensen, W. L. Evaluation and reparametrization of the OPLS-AA force field for proteins via comparison with accurate quantum chemical calculations on peptides. *J. Phys. Chem. B* **2001**, *105*, 6474–6487.
- (51) Still, W. C.; Tempczyk, A.; Hawley, R. C.; Hendrickson, T. Semianalytical treatment of solvation for molecular mechanics and dynamics. *J. Am. Chem. Soc.* **1990**, *112*, 6127–6129.
- (52) Tavelin, S.; Gråsjö, J.; Taipalensuu, J.; Ocklind, G.; Artursson, P. Applications of epithelial cell culture in studies of drug transport. *Methods Mol. Biol.* **2002**, *188*, 233–272.